Universal link of magnetic exchange and structural behavior under pressure in chromium spinels

Ilias Efthimiopoulos[a,b,1,2], *Indiras Khatri*[c,2], *Zhi T. Y. Liu*[c], *Sanjay V. Khare*[c], *Pankaj Sarin*[d], *Vladimir Tsurkan*[e], *Alois Loidl*[e], *Dongzhou Zhang*[f], *and Yuejian Wang*[a,1]

[a]Department of Physics, Oakland University, Rochester, Michigan 48309, USA

[b]Deutsches GeoForschungsZentrum, Section 4.3, Telegrafenberg, 14473, Potsdam, Germany

[c]Department of Physics and Astronomy, University of Toledo, Toledo, Ohio 43606, USA

[d]School of Materials Science and Engineering, Oklahoma State University, Tulsa, Oklahoma 74106, USA

[e]E. P. V, Center for Electronic Correlations and Magnetism, University of Augsburg, 86159 Augsburg, Germany

[f]Partnership for Extreme Crystallography, University of Hawaii at Manoa, Honolulu, Hawaii 96822, USA

SUPPLEMENTARY INFORMATION

Supplementary Information Text

We present here the complete set of experimental structural parameters, as well as lists of detailed structural and magnetic data used for our DFT calculations. An overview Table for all relevant spinels are supplied also for convenience.

Additional details on methods

XRD refinements. Most of the XRD patterns were fitted with the Rietveld method. The refined parameters in each case were the lattice parameters, the atomic coordinates (Mn, Ni, and Cr reside in fixed positions in the ambient-pressure structures), and the profile parameters of the Stephens peak function[1], whereas the background was modelled with a Chebyshev polynomial. Since the diffractograms showed textured rings, we employed a spherical harmonics correction[2] in order to account for the preferred orientation of the powder particles. All of the Rietveld refinements were performed with spherical harmonic orders of 6 for both phases. The weighted residuals of the Rietveld fits wR_p and the reduced χ^2 parameters ("goodness of the fit") varied between 0.5 – 1.5 % and 0.01 – 0.2 for all XRD refinements, respectively. We should mention that the isotropic atomic displacement parameters U_{iso} for both the $I4_1/amd$ and $Fd\bar{3}m$ phases were found to be pressure insensitive, hence they were fixed to their refined ambient-pressure values (see footnotes). Finally, the high-pressure tetragonal modifications of $MnCr_2O_4$ were fitted with the Le Bail method, i.e. only the lattice parameters were extracted.

DFT calculations. The density function theory (DFT) based calculations have been performed with the Vienna Ab initio simulation package[3–6]. Potentials of Cr_pv, Mn_pv, Fe, Co, Ni_pv, Cu_pv and O using projector-augmented wave method[7,8] were selected, with the Perdew-Burke-Ernzerhof PBE generalized gradient approximation (GGA)[9]. The U values were chosen to be 3.7 eV for Cr, 3.9 eV for Mn, 5.3 eV for Fe, 3.32 eV for Co, and 6.2 eV for Ni[10,11]. The plane wave cutoff energy was chosen to be 550 eV to ensure lattice parameter relaxations. The k-point meshes were created with k points per reciprocal atoms (KPPRA) of 4000. During the electronic iterations, Gaussian smearing was used with a sigma value as small as 0.05 eV, until the convergence criterion of 10-4 eV was reached. We note that we used the experimental structure of the $I4_1/amd$ tetragonal phase for both $NiCr_2O_4$ and $CuCr_2O_4$ for the DFT calculations. To determine the magnetic exchange interactions parameters, we have calculated the total energies for different magnetic configurations. The exchange parameters are then obtained by using the classical Heisenberg model.

$$\Delta E = -\sum_{i,j} J_{ij} \hat{e_i} . \hat{e_j}$$

where, J_{ij} is the magnetic exchange interactions parameter and $\hat{e_i}$ and $\hat{e_j}$ are the unit vectors pointing in the direction of the magnetic moments at the sites i and j, respectively.

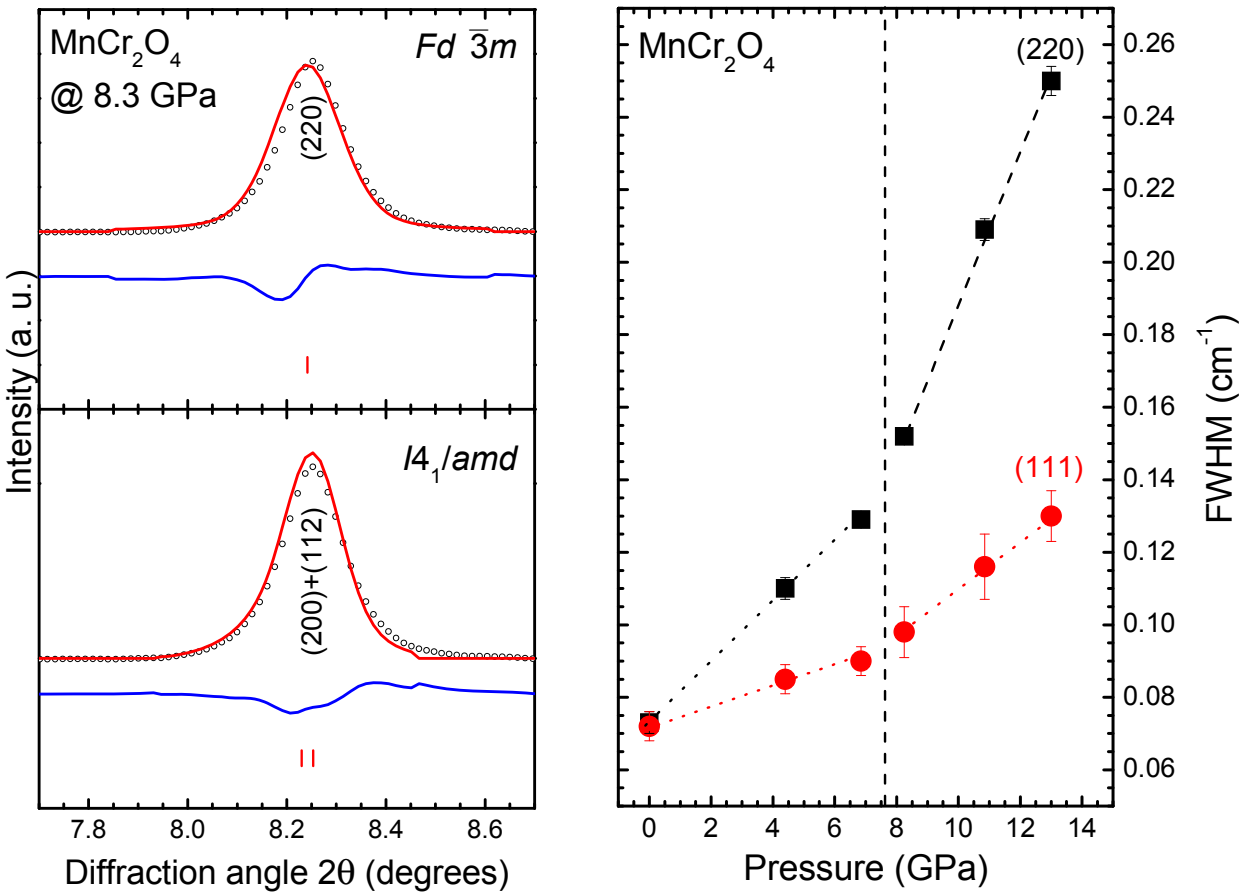

Fig. S1: (Left) Enhanced view of the 7.6°-8.8° 2θ region of the $MnCr_2O_4$ XRD pattern at 8.3 GPa. Dots stand for the measured spectra, the red solid lines represent the refinements, and their difference is drawn as blue lines. Vertical ticks mark Bragg peak positions. Notice the better refinement result assuming a tetragonal structure (in this case: SG $I4_1/amd$) over the original cubic one (SG $Fd\bar{3}m$). (Right) Evolution of the full width at half-maximum (FWHM) for selected Bragg peaks of $MnCr_2O_4$ as a function of pressure. The vertical dashed line represents the change in the pressure rate, whereas the dotted lines serve as guides for the eye.

Table S1: Structural data for the $Fd\bar{3}m$ (Z = 8) and the high-pressure tetragonal phases (Z = 4) of $MnCr_2O_4$.

$Fd\bar{3}m$ [a]	P (GPa)	a (Å)	V (Å^3)	O-u	Mn-O (Å)	Cr-O (Å)
	Ambient	8.4431(1)	601.9	0.2642(2)	2.04(1)	2.00(1)
	4.4	8.3830(1)	589.1	0.2634(2)	2.01(1)	1.99(1)
	6.9	8.3572(1)	583.7	0.2640(2)	2.01(1)	1.98(1)
Tetragonal HP 1	P (GPa)	a (Å)	c (Å)	$c/a\sqrt{2}$	V (Å^3)	
	8.3	5.9510(1)	8.1862(5)	0.973	289.9	
	10.9	5.9376(1)	8.1452(5)	0.97	287.2	
	13	5.9302(1)	8.1005(5)	0.966	284.8	
	14.9	5.9250(1)	8.0619(5)	0.962	283	
	17.2	5.9172 (1)	8.0245(5)	0.959	281	
	19.2	5.9100(1)	7.9825(5)	0.955	278.8	
Tetragonal HP 2	P (GPa)	a (Å)	c (Å)	$c/a\sqrt{2}$	V (Å^3)	
	21.1	6.1411(5)	7.3497(7)	0.846	277.2	
	24.3	6.1388(5)	7.2519(7)	0.835	273.3	
	26.1	6.1365(5)	7.2007(7)	0.83	271.1	
	29.2	6.1341(5)	7.1395(7)	0.823	268.6	
	31.7	6.1321(5)	7.0709(7)	0.815	265.9	
	34.1	6.1302(5)	7.0113(7)	0.809	263.5	

Table S1. Footnotes

[a] **Wyckoff positions:** Mn (8a: 0.125, 0.125, 0.125), Cr (16d: 0.5, 0.5, 0.5), O (32e: u, u, u)
Isotropic atomic displacement parameters U_{iso}: $U_{iso,Mn}$ = 0.01(1) Å^2, $U_{iso,Cr}$ = 0.03(1) Å^2, $U_{iso,O}$ = 0.04(1) Å^2

Table S2: DFT-calculated structural parameters for the $Fd\bar{3}m$ (Z = 8) and the high-pressure tetragonal modifications (Z = 4) of $MnCr_2O_4$.

Phase	***P* (GPa)**	***a* (Å)**	***V* (Å^3)**	**Energy (eV)**		
Fd*$\bar{3}$*m	-5.85	8.7163	660.00	-445.54		
	-3.11	8.6647	647.78	-445.88		
	-0.10	8.6060	635.56	-446.00		
	3.21	8.5548	623.33	-445.89		
	6.86	8.4967	611.11	-445.51		
	10.87	8.4407	598.89	-444.83		
	15.29	8.3881	586.67	-443.83		
	20.17	8.3320	574.44	-442.48		
	25.55	8.2672	562.22	-440.75		
	31.50	8.2225	550.00	-438.57		
Phase	***P* (GPa)**	***a* (Å)**	***c* (Å)**	***c*/*a*√2**	***V* (Å^3)**	**Energy (eV)**
$I4_1/amd$	-6.93	6.1832	8.7119	0.9963	333.07	-222.646
AFM-MnCr	-4.59	6.1479	8.6629	0.9964	327.43	-222.851
	-2.03	6.1129	8.6114	0.9961	321.79	-222.970
	0.79	6.0798	8.5526	0.9947	316.14	-222.992
	3.88	6.0423	8.5046	0.9953	310.50	-222.910
	7.28	6.0053	8.4533	0.9954	304.86	-222.711
	11.02	5.9691	8.3977	0.9948	299.21	-222.389
	15.13	5.9318	8.3432	0.9946	293.57	-221.931
	19.65	5.8936	8.2894	0.9946	287.93	-221.325
	24.63	5.8541	8.2369	0.9949	282.29	-220.547
	30.13	5.8135	8.1855	0.9956	276.64	-219.578
Phase	***P* (GPa)**	***a* (Å)**	***c* (Å)**	***c*/*a*√2**	***V* (Å^3)**	**Energy(eV)**
$I4_1/amd$	-5.40	6.1864	8.6988	0.9943	333.07	-222.622
AFM-Cr	-3.61	6.1503	8.6521	0.9947	327.43	-222.828
	-1.55	6.1168	8.5967	0.9938	321.79	-222.948
	0.83	6.0793	8.5494	0.9944	316.14	-222.970
	3.55	6.0454	8.4902	0.9931	310.50	-222.887
	6.67	6.0064	8.4450	0.9942	304.86	-222.688
	10.24	5.9701	8.3895	0.9937	299.21	-222.365
	14.31	5.9442	8.3013	0.9875	293.57	-221.910
	18.96	5.9210	8.2093	0.9804	287.93	-221.304
	24.27	5.8913	8.1359	0.9765	282.29	-220.526
	30.33	5.8775	8.0072	0.9633	276.64	-219.576
	34.07	6.0655	7.4211	0.8651	273.50	-219.111
	37.24	6.1307	7.1943	0.8298	271.00	-218.717

Table S3: Construction parameters (lattice vectors and Fractional coordinates) for special quasi-random paramagnetic $MnCr_2O_4$ supercell. The first half of Mn and Cr cations are set spin-up, and the second half spin-down.

Lattice Vector (Å)	**x**	**y**	**z**
a	8.49	0	0
b	0	8.49	0
c	0	0	8.49

	Fractional Coordinates				**Fractional Coordinates**		
Ions	**u_1**	**u_2**	**u_3**	**Ions**	**u_1**	**u_2**	**u_3**
Mn	0.000000	0.000000	0.500000	O	0.113711	0.886289	0.113711
Mn	0.750000	0.750000	0.750000	O	0.113711	0.113711	0.886289
Mn	0.000000	0.500000	0.000000	O	0.886289	0.613711	0.613711
Mn	0.750000	0.250000	0.250000	O	0.886289	0.386289	0.386289
Mn	0.500000	0.000000	0.000000	O	0.636289	0.636289	0.363711
Mn	0.250000	0.750000	0.250000	O	0.136289	0.363711	0.136289
Mn	0.500000	0.500000	0.500000	O	0.863711	0.636289	0.136289
Mn	0.250000	0.250000	0.750000	O	0.363711	0.363711	0.363711
Cr	0.625000	0.125000	0.625000	O	0.113711	0.386289	0.613711
Cr	0.375000	0.875000	0.625000	O	0.113711	0.613711	0.386289
Cr	0.875000	0.125000	0.875000	O	0.386289	0.113711	0.613711
Cr	0.125000	0.875000	0.875000	O	0.386289	0.886289	0.386289
Cr	0.625000	0.625000	0.125000	O	0.136289	0.136289	0.363711
Cr	0.375000	0.375000	0.125000	O	0.636289	0.863711	0.136289
Cr	0.875000	0.625000	0.375000	O	0.363711	0.136289	0.136289
Cr	0.125000	0.375000	0.375000	O	0.863711	0.863711	0.363711
Cr	0.125000	0.125000	0.125000	O	0.613711	0.886289	0.613711
Cr	0.875000	0.875000	0.125000	O	0.613711	0.113711	0.386289
Cr	0.375000	0.125000	0.375000	O	0.386289	0.613711	0.113711
Cr	0.625000	0.875000	0.375000	O	0.386289	0.386289	0.886289
Cr	0.125000	0.625000	0.625000	O	0.136289	0.636289	0.863711
Cr	0.875000	0.375000	0.625000	O	0.636289	0.363711	0.636289
Cr	0.375000	0.625000	0.875000	O	0.363711	0.636289	0.636289
Cr	0.625000	0.375000	0.875000	O	0.863711	0.363711	0.863711
O	0.886289	0.113711	0.113711	O	0.613711	0.386289	0.113711
O	0.886289	0.886289	0.886289	O	0.613711	0.613711	0.886289
O	0.636289	0.136289	0.863711				
O	0.136289	0.863711	0.636289				
O	0.863711	0.136289	0.636289				
O	0.363711	0.863711	0.863711				

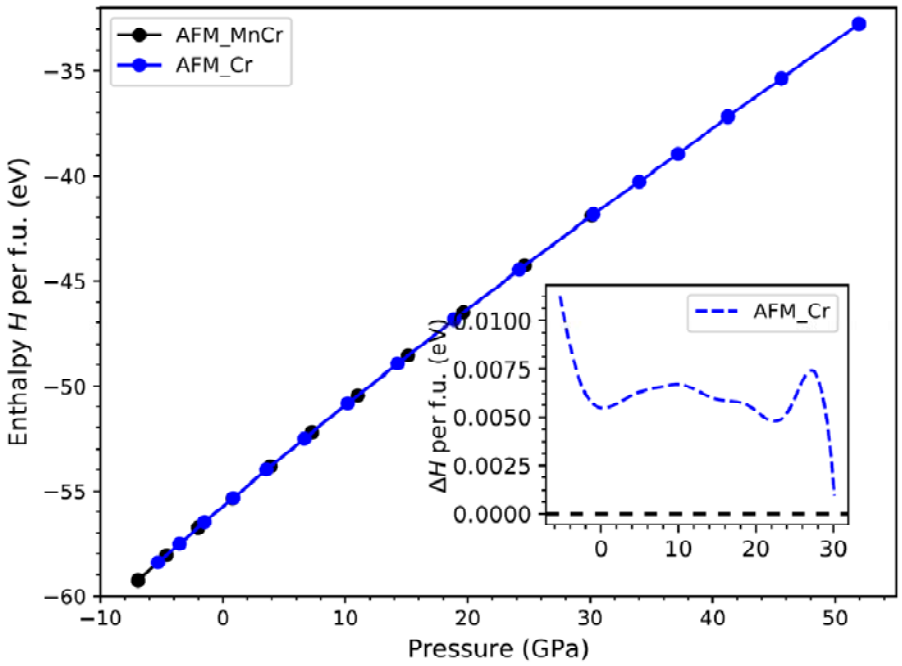

Fig. S2: The calculated enthalpies of the the tetragonal AFM1 (AFM-MnCr, black) and tetragonal AFM2 (AFM-Cr, blue) phases as a function of pressure. Inset: the enthalpy difference between the tetragonal AFM1 and AFM2 phases and the cubic phase with respect to pressure. Enthalpy H is defined as $H(P) = E + PV$, and a lower value of H indicates the phase stability. The AFM-MnCr→AFM-Cr transition is expected to take place at 30.5 GPa (extrapolated in bottom plot, the experimental value is 21.1 GPa).

Table S4: Structural data for the $I4_1/amd$ ($Z = 4$) and the high-pressure $P4_32_12$ ($Z = 8$) tetragonal phases of $NiCr_2O_4$.

$I4_1/amd$ [a]	P (GPa)	a (Å)	c (Å)	$c/a\sqrt{2}$	V (Å^3)	O-y	O-z	Ni-O (Å)	Cr-O(//ab) (Å)	Cr-O(//c) (Å)	Cr-O(//ab//c)
	10^{-4}	5.8365(1)	8.4475(1)	1.023	287.8	0.0219(4)	0.7704(4)	2.007(1)	1.982(2)	1.944(3)	0.981
	1.2	5.8108(1)	8.4715(1)	1.031	286	0.0174(2)	0.7677(2)	1.969(3)	1.990(3)	1.971(3)	0.99
	4.3	5.7539(1)	8.5016(1)	1.045	281.5	0.0189(2)	0.7690(3)	1.973(3)	1.965(3)	1.967(3)	1.001
	6.9	5.7180(1)	8.5071(1)	1.052	278.1	0.0152(2)	0.7680(2)	1.944(3)	1.967(2)	1.976(3)	1.004
	9.6	5.6820(1)	8.5075(1)	1.059	274.7	0.0162(3)	0.7691(4)	1.947(3)	1.952(2)	1.966(3)	1.007
	12.9	5.6408(1)	8.5038(1)	1.066	270.6	0.0159(3)	0.7703(3)	1.943(2)	1.940(4)	1.955(3)	1.008
	16.6	5.5957(1)	8.4892(1)	1.073	265.8	0.0159(2)	0.7702(4)	1.932(2)	1.924(4)	1.953(3)	1.016
	19.4	5.5550(1)	8.4710(1)	1.078	261.1	-	-	-	-	-	-

$P4_32_12$ [b]	P (GPa)	a (Å)	c (Å)	c/a	V (Å^3)	Ni-x	Ni-y	Ni-z	Cr(1)-x	Cr(2)-x	Cr(3)-x	Cr(3)-y	Cr(3)-z	O(1)-x	O(1)-y	O(1)-z	O(2)-x	O(2)-y	O(2)-z	O(3)-x	O(3)-y	O(3)-z	O(4)-x	O(4)-y	O(4)-z
	19.4	8.4489(1)	7.1718(2)	0.849	511.9	-	-	-	-	-	-	-	-	-	-	-	-	-	-	-	-	-	-	-	-
	23.2	8.4304(1)	7.0659(3)	0.838	502.2	0.3443(2)	0.8768(3)	0.0166(3)	0.6440(4)	0.1225(4)	0.2554(3)	0.0105(4)	0.6033(3)	0.1403(3)	0.8937(4)	-0.0322(4)	0.5907(5)	0.3847(3)	-0.0071(6)	0.3141(5)	0.0717(6)	0.0504(4)	1.0221(5)	0.5550(4)	-0.1808(5)
	26	8.4274(1)	6.9742(3)	0.828	495.3	0.3563(2)	0.8655(3)	0.0258(3)	0.6500(4)	0.1150(4)	0.2546(3)	-0.0008(4)	0.6120(3)	0.1585(4)	0.8955(4)	-0.0419(4)	0.6059(4)	0.3710(3)	-0.0163(6)	0.2865(5)	0.0788(8)	0.0535(4)	1.0398(5)	0.5857(4)	-0.2028(5)
	29.7	8.4173(1)	6.8772(2)	0.817	487.3	0.3565(2)	0.8716(3)	0.0300(3)	0.6533(4)	0.1173(4)	0.2516(3)	0.0015(4)	0.6293(3)	0.1187(4)	0.8803(4)	-0.0141(4)	0.6446(5)	0.3922(4)	0.0225(6)	0.3107(5)	0.0656(8)	-0.0110(4)	1.0635(5)	0.5742(4)	-0.0954(6)
	32.5	8.4029(1)	6.8169(4)	0.811	481.3	0.3593(2)	0.8699(3)	0.0370(3)	0.6627(4)	0.1157(4)	0.2412(3)	-0.0048(4)	0.6317(3)	0.1297(4)	0.8805(5)	-0.0067(4)	0.6561(4)	0.4165(4)	0.0236(6)	0.3290(5)	0.0757(8)	-0.0491(4)	1.0670(5)	0.5835(4)	-0.0536(7)
	36.1	8.3884(1)	6.7477(3)	0.804	474.8	0.3466(2)	0.8843(3)	0.0250(2)	0.6287(4)	0.1323(4)	0.2246(3)	-0.0012(4)	0.6180(3)	0.1292(4)	0.9156(4)	-0.0399(4)	0.6335(5)	0.3502(4)	0.0222(5)	0.3673(6)	0.1022(8)	0.0589(4)	0.9168(5)	0.5893(6)	-0.0956(7)
	39.8	8.3704(2)	6.6711(3)	0.797	467.4	0.3521(2)	0.8896(2)	0.0427(2)	0.6039(4)	0.1235(4)	0.2561(3)	-0.0009(4)	0.6083(3)	0.1116(4)	0.9088(5)	-0.0009(4)	0.6708(6)	0.3785(4)	-0.0067(5)	0.3257(6)	0.1516(8)	-0.0910(4)	0.8744(5)	0.5371(8)	-0.1186(7)
	42.9	8.3502(2)	6.6280(3)	0.794	462.1	0.3499(2)	0.8874(2)	0.0418(2)	0.6189(4)	0.1371(4)	0.2534(3)	-0.0129(4)	0.5873(3)	0.1816(4)	0.9221(5)	-0.0383(4)	0.6125(6)	0.3868(4)	-0.0037(5)	0.3222(6)	0.1600(8)	-0.0465(5)	0.9275(5)	0.5697(8)	-0.1172(8)
	46.3	8.3316(3)	6.5920(2)	0.791	457.6	0.3403(2)	0.8891(2)	0.0413(2)	0.6158(4)	0.1391(4)	0.2600(3)	-0.0139(4)	0.5798(3)	0.1702(4)	0.9279(5)	-0.0582(5)	0.6127(6)	0.3943(5)	-0.0236(6)	0.3180(6)	0.1525(8)	-0.0456(6)	0.9398(5)	0.5681(8)	-0.1177(9)
	50.2	8.3142(2)	6.5462(4)	0.787	452.5	0.3391(2)	0.8884(2)	0.0371(2)	0.6201(4)	0.1339(4)	0.2561(3)	-0.0015(4)	0.5869(3)	0.167(4)	0.942(5)	-0.071(5)	0.634(6)	0.392(5)	-0.009(6)	0.319(6)	0.166(4)	-0.056(7)	0.940 (5)	0.563(3)	-0.073(1)

Table S4. Footnotes

[a] **Wyckoff positions:** Ni (4b: 0, 0.25, 0.375), Cr (8c: 0, 0, 0), O (16h: 0, y, z); **Isotropic atomic displacement parameters U_{iso}**: $U_{iso,Ni}$ = 0.02(1) Å^2, $U_{iso,Cr}$ = 0.04(1) Å^2, $U_{iso,O}$ = 0.03(1) Å^2

[b] **Wyckoff positions:** Ni (8b: x, y, z), Cr(1) (4a: x, x, 0), Cr(2) (4a: x, x, 0), Cr(3) (8b: x, y, z), O(1) (8b: x, y, z), O(2) (8b: x, y, z), O(3) (8b: x, y, z), O(4) (8b: x, y, z); **Isotropic atomic displacement parameters U_{iso}**: $U_{iso,Ni}$ = 0.003(1) Å^2, $U_{iso,Cr}$ = 0.004(1) Å^2, $U_{iso,O}$= 0.006(1) Å^2

Table S5: DFT-calculated structural parameters for the phases of $NiCr_2O_4$.

$I4_1/amd$-paraM					$I4_1/amd$-AFM				
***P* (GPa)**	***a* (Å)**	***c* (Å)**	***c*/*a****	***V* (Å^3)**	***P* (GPa)**	***a* (Å)**	***c* (Å)**	***c*/*a****	**V (Å^3)**
-8.4222	6.0953	8.6869	1.0077	320	-8.7021	6.0087	8.8611	1.0428	320.00
-5.7029	6.0563	8.6434	1.0092	314.55	-6.3205	5.9621	8.8509	1.0497	314.55
-2.8244	6.0121	8.6120	1.0129	309.09	-3.7330	5.9160	8.8326	1.0557	309.09
0.2204	5.9673	8.5824	1.0170	303.64	-0.9212	5.8791	8.7813	1.0562	303.64
3.4385	5.9309	8.5305	1.0170	298.18	2.1351	5.8405	8.7425	1.0584	298.18
6.8370	5.8956	8.4806	1.0171	292.73	5.4585	5.8014	8.7004	1.0605	292.73
10.4225	5.8467	8.4563	1.0227	287.27	9.0735	5.7499	8.6897	1.0686	287.27
14.2009	5.7933	8.4491	1.0313	281.82	13.0076	5.7085	8.6544	1.0720	281.82
18.1777	5.7211	8.4636	1.0461	276.36	17.2912	5.6526	8.6462	1.0816	276.36
22.3571	5.6549	8.4750	1.0597	270.91	21.9579	5.6095	8.6056	1.0848	270.91
26.7421	5.5866	8.4827	1.0737	265.45	27.0454	5.5507	8.6169	1.0977	265.45
29.2458	5.5531	8.4936	1.0815	262.45	30.0425	5.5184	8.6148	1.1039	262.45
31.3337	5.5191	8.4944	1.0883	260	32.5955	5.4964	8.6040	1.1069	260.00
38.7586	5.4114	8.4940	1.1099	251.65	39.9969	5.4328	8.5871	1.1177	253.40
47.5889	5.2726	8.4760	1.1367	242.33	50.0164	5.3508	8.5772	1.1335	245.47
$P4_32_12$-ParaM					$P4_32_12$-AFM				
***P* (GPa)**	***a* (Å)**	***c* (Å)**	***c*/*a***	***V* (Å^3)**	***P* (GPa)**	***a* (Å)**	***c* (Å)**	***c*/*a***	***V* (Å^3)**
-3.6602	9.0227	7.3679	0.8166	600.0000	-4.8551	8.9902	7.4596	0.8298	600
-1.9566	8.9740	7.2638	0.8094	585.0000	-1.5306	8.9435	7.3499	0.8218	585
0.4627	8.9155	7.1715	0.8044	570.0000	2.2990	8.8954	7.2408	0.8140	570
3.7655	8.8527	7.0800	0.7998	555.0000	6.7134	8.8418	7.1347	0.8069	555
8.1581	8.7974	6.9744	0.7928	540.0000	11.8067	8.7940	7.0175	0.7980	540
13.8952	8.7381	6.8792	0.7873	525.0000	17.6901	8.7350	6.9138	0.7915	525
16.1588	8.7088	6.8594	0.7876	520.0000	19.8492	8.7125	6.8830	0.7900	520
18.6197	8.6873	6.8287	0.7861	515.0000	22.1162	8.6957	6.8422	0.7869	515
21.2924	8.6641	6.7961	0.7844	510.0000	24.4970	8.6772	6.8051	0.7843	510
24.1922	8.6398	6.7655	0.7831	505.0000	26.9977	8.6567	6.7686	0.7819	505
27.3360	8.6149	6.7366	0.7820	500.0000	29.6251	8.6357	6.7342	0.7798	500
30.7417	8.5903	6.7081	0.7809	495.0000	32.3863	8.6174	6.6943	0.7768	495
34.4289	8.5698	6.6731	0.7787	490.0000	35.2886	8.5998	6.6555	0.7739	490
38.4185	8.5426	6.6405	0.7773	485.0000	38.3402	8.5743	6.6246	0.7726	485
42.7328	8.5240	6.6034	0.7747	480.0000	41.5494	8.5541	6.5863	0.7700	480
47.3965	8.5002	6.5719	0.7731	475.0000	44.9257	8.5295	6.5540	0.7684	475
52.4358	8.4784	6.5348	0.7708	470.0000	48.4783	8.5080	6.5189	0.7662	470
57.8792	8.4520	6.5056	0.7697	465.0000	52.2180	8.4885	6.4792	0.7633	465
					56.1556	8.4635	6.4452	0.7615	460

Table S6: The experimental structure of $NiCr_2O_4$ (Space group: $I4_1/amd$) used in the calculations.

Lattice vector (Å)	x	y	Z
a	5.84	0	0
b	0	5.84	0
c	0	0	8.43

Fractional Coordinates

Ions	**u_1**	**u_2**	**u_3**
Ni	0.000000000	0.250000000	0.375000000
Ni	0.000000000	0.750000000	0.625000000
Ni	0.500000000	0.750000000	0.875000000
Ni	0.500000000	0.250000000	0.125000000
Cr	0.000000000	0.000000000	0.000000000
Cr	0.500000000	0.000000000	0.500000000
Cr	0.250000000	0.750000000	0.250000000
Cr	0.750000000	0.250000000	0.750000000
Cr	0.250000000	0.250000000	0.750000000
Cr	0.750000000	0.750000000	0.250000000
Cr	0.500000000	0.500000000	0.500000000
Cr	0.000000000	0.500000000	0.000000000
O	0.000000000	0.505999982	0.238700002
O	0.000000000	0.494000018	0.761299968
O	0.500000000	0.494000018	0.738700032
O	0.500000000	0.505999982	0.261299998
O	0.744000018	0.750000000	0.488700002
O	0.255999982	0.250000000	0.511299968
O	0.755999982	0.250000000	0.988700032
O	0.244000018	0.750000000	0.011299998
O	0.755999982	0.750000000	0.011299998
O	0.244000018	0.250000000	0.988700032
O	0.744000018	0.250000000	0.511299968
O	0.255999982	0.750000000	0.488700002
O	0.500000000	0.005999982	0.738700032
O	0.500000000	0.994000018	0.261299998
O	0.000000000	0.994000018	0.238700002
O	0.000000000	0.005999982	0.761299968

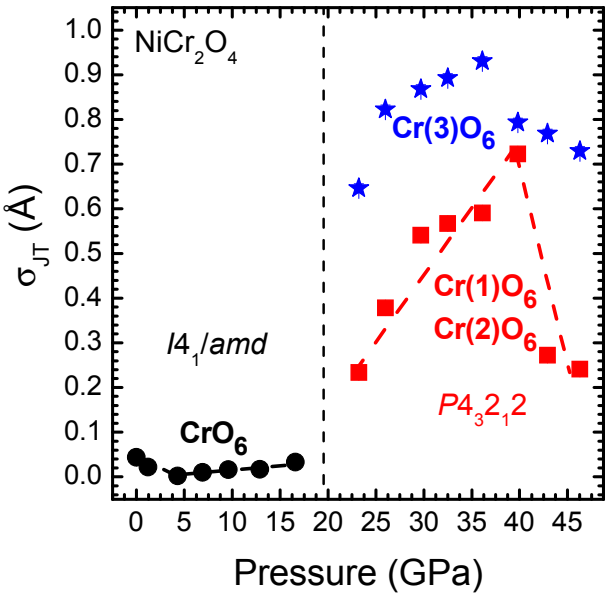

Fig. S3: The Jahn-Teller distortion parameter σ_{JT}, as calculated from our XRD data for the CrO_6 octahedra of the $I4_1/amd$ and high-pressure $P4_32_12$ phases of $NiCr_2O_4$. The parameter is defined as $\sigma_{JT} = \sqrt{\sum_{i=1}^{6}[(Cr-O)_i - \langle Cr-O\rangle]^2}$, where (Cr-O)$_i$ are the six different Cr-O bond distances, and <Cr-O> the average value of the Cr-O bond lengths[12]. Notice that there are three different CrO_6 octahedra in the $P4_32_12$ modification.

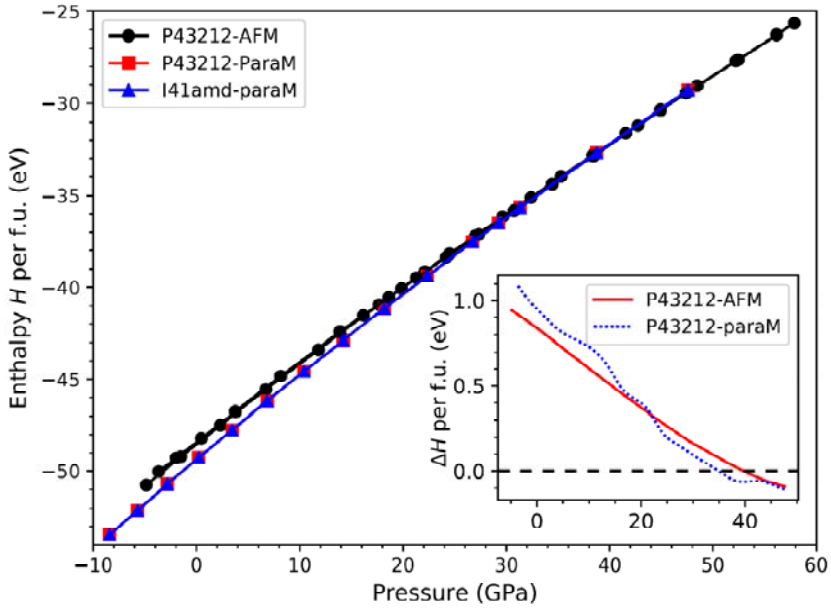

Fig. S4: The calculated enthalpies of the $P4_32_12$-AFM (black), the $P4_32_12$-ParaM (red) and $I4_1/amd$ (ParaM, blue) phases as a function of pressure. Inset: the enthalpy difference between the $P4_32_12$ (AFM and paraM) and $I4_1/amd$ (paraM) phases with respect to pressure. Enthalpy H is defined as $H(P) = E + PV$, and a phase is stable if it has a lower value of H. The $I4_1/amd$-paraM→ $P4_32_12$-ParaM transition is calculated at 35 GPa. The $I4_1/amd$-paraM→ $P4_32_12$-AFM transition is estimated at 40 GPa.

Table S7: Calculation of magnetic exchange parameters of different spinels A = [Mn, Fe, Co, Ni, Cu] and B = [Cr].

The Classical Heisenberg equation used to calculate the magnetic exchange parameters is:

$$E = E_0 + C_{AA}J_{AA} + C_{AB}J_{AB} + C_{BB}J_{BB}$$

where, C_{AA}, C_{AB} and C_{BB} are the coefficients of the Heisenberg model. The Following tables are the Magnetic moment construction and the summations of the Heisenberg model [13,14] employed for the determination of the magnetic exchange parameters J_{AA}, J_{AB}, J_{BB} of:

(A) The structure used is 8 times the unit cell of $MnCr_2O_4$

Magnetic configurations	**Mn**	**Cr**
Ferromagnetic	All Up	All Up
Neel-type Ferrimagnetic	All Down	All Up
Disorder-1	All UP	8 Up & 8 Down
Disorder-2	3 Down & 5 Up	4 Down & 12 Up

Magnetic configuration	$C_{Mn\text{-}Mn}$	$C_{Mn\text{-}Cr}$	$C_{Cr\text{-}Cr}$
Ferromagnetic	16	96	48
Neel-type Ferrimagnetic	16	-96	48
Disorder-1	16	0	-16
Disorder-2	0	16	16

(B) The structure used is 4 times the unit cell of $NiCr_2O_4$

Magnetic configurations	**Ni**	**Cr**
Ferromagnetic	All Up	All Up
Neel-type Ferrimagnetic	All Down	All Up
Ferrimagnetic in Cr	All Up	2 Up 2 Down 2 Up 2 Down
Disorder-1	1 Up 3 Down	6 Up 2 Down
Disorder-2	3 Down 1 Up	5 Up 3 Down
Disorder-3	3 Down 1 Up	5 Up 4 Down

Magnetic configuration	$C_{Ni\text{-}Ni}$	$C_{Ni\text{-}Cr}$	$C_{Ni\text{-}Ni}$
Ferromagnetic	8	48	24
Neel-type ferrimagnetic	8	-48	24
Ferrimagnetic in Cr	8	0	-8
Disorder-1	0	-12	0
Disorder-2	0	-8	-4
Disorder-3	0	0	-8

(C) The structure used is 8 times the unit cell of $FeCr_2O_4$.

Magnetic configurations	**Fe**	**Cr**
Ferromagnetic	All Up	All Up
Neel-type Ferrimagnetic	All Down	All Up
Ferrimagnetic in Cr	All Up	2 Up 2 Down 2 Up 2 Down 2 Up 2 Down 2 Up 2 Down
Ferrimagnetic in Fe	2 Up 2 Down 2 Up 2 Down	All Up

Magnetic configuration	$\mathbf{C_{Fe-Fe}}$	$\mathbf{C_{Fe-Cr}}$	$\mathbf{C_{Cr-Cr}}$
Ferromagnetic	16	96	48
Neel-type Ferrimagnetic	16	-96	48
Ferrimagnetic in Cr	16	0	-16
Ferrimagnetic in Fe	0	0	48

(**D**) The structure used is 8 times the unit cell of $CoCr_2O_4$.

Magnetic configurations	**Co**	**Cr**
Ferromagnetic	All Up	All Up
Neel-type Ferrimagnetic	All Down	All Up
Ferrimagnetic in Cr	All Up	2 Up 2 Down 2 Up 2 Down 2 Up 2 Down 2 Up 2 Down
Disorder-1	3 Down 5 Up	4 Down 12 Up
Disorder-2	7 Up 1 Down	All Up

Magnetic configuration	$\mathbf{C_{Co-Co}}$	$\mathbf{C_{Co-Cr}}$	$\mathbf{C_{Cr-Cr}}$
Ferromagnetic	16	96	48
Neel-type Ferrimagnetic	16	-96	48
Ferrimagnetic in Cr	16	0	-16
Disorder-1	0	16	16
Disorder-2	4	16	16

(**E**) The structure used is 4 times the unit cell of $CuCr_2O_4$

Magnetic configuration	**Cu**	**Cr**
Ferromagnetic	All Up	All Down
Ferrimagnetic in Cr	All Up	2 Up 2 Down 2 Up 2 Down
Disorder-1	1 Down 3 Up	6 Up 2 Down
Disorder-2	3 Down 1 Up	5 Up 3 Down
Disorder-3	3 Down 1 Up	4 Up 4 Down
Disorder-4	All Up	7 Up 1 Down
Disorder-5	1 Down 3 Up	7 Up 1 Down

Magnetic configuration	$\mathbf{C_{Cu\text{-}Cu}}$	$\mathbf{C_{Cu\text{-}Cr}}$	$\mathbf{C_{Cr\text{-}Cr}}$
Ferromagnetic	8	48	24
Ferrimagnetic in Cr	8	-48	24
Disorder-1	8	0	-8
Disorder-2	0	12	0
Disorder-3	0	-8	-4
Disorder-4	0	0	-8
Disorder-5	0	16	12

Table S8: Transition pressures (P_{Tr}), the various magnetic exchange parameters, ratios, and the respective results from the literature for the various Cr-bearing spinels with magnetic A^{2+} cations (A^{2+} = Mn, Fe, Co, Ni, Cu). The abbreviations stand for: N/A = not available, GGA = Generalized gradient approximation, LSDA = local spin density approximation, and χ = magnetic susceptibility.

Compound	P_{Tr} (GPa)	J_{AA} (meV)	J_{AB} (meV)	J_{BB} (meV)	J_{AA}/J_{BB}	J_{AB}/J_{BB}	Comp. Method	U_A (eV)	U_{Cr} (eV)	Ref.
$MnCr_2O_4$	11	-2.59	-0.72	-0.96	2.70	0.75	GGA+U	3.9	3.7	Here
(MCO)		-1.58	-1.47	-1.28	1.23	1.15	GGA+U	4	3	[15]
		-0.42	-0.67	-2.08	0.20	0.32	Fitting χ	N/A	N/A	[16]
		-1.5	-3	-2	0.75	1.50	LSDA+U	4	4	[13]
$FeCr_2O_4$	12	-1.98	-1.86	-2.23	0.89	0.83	GGA+U	5.3	3.7	Here
(FCO)		-0.67	-2.88	-2.83	0.24	1.02	GGA+U	5	3	[15]
$CoCr_2O_4$	16	-2.73	-4.54	-2.78	0.98	1.63	GGA+U	3.32	3.7	Here
(CCO)		-0.56	-3.01	-3.26	0.17	0.92	GGA+U	5	3	[15]
		N/A	N/A	-3	0.55(5)	1.02(1)	Monte Carlo & fitting χ	N/A	N/A	[17]
		-1	-4	-2	0.5	2	LSDA+U	3	4	[13]
		-0.92	-9	-2.97	0.31	3.03	GGA+U[a]	3.3	3.7	[14]
$NiCr_2O_4$	25	-2.13	-3.84	-4.29	0.50	0.89	GGA+U	6.2	3.7	Here
(NCO)		-1.64	-5.36	-3.94	0.42	1.36	GGA+U	5	3	[15]
$CuCr_2O_4$ (CuCO)	25	-15.92	-3.14	-15.2627	1.04	0.21	GGA+U	0	3.7	Here

[a] In earlier calculations reported in Ref. 14, we noticed the incorrect counting of the total number of interactions between Co-Cr in $CoCr_2O_4$ [instead of 24 interactions as listed in **Table S5** in the Supplement of Ref. 15, there are 48 of them]. While calculating the exchange interaction parameters we used more than four configurations, and we accepted those values of J_{AA}, J_{AB}, and J_{BB} which have minimum errors. Hence, the main reason behind the magnetic exchange numerical values discrepancy in our paper and those of Ref. 14 could be the incorrect counting of the total number of interactions between Co-Cr in the previous calculations of Ref. 14.

REFERENCES for SI

[1] P.W. Stephens, J. Appl. Cryst. **32**, 281 (1999).
[2] R.B. von Dreele, J. Appl. Cryst. **30**, 517 (1997).
[3] G. Kresse and J. Furthmuller, Comput. Mater. Sci. **6**, 15 (1996).
[4] G. Kresse and J. Furthmüller, Phys. Rev. B **54**, 11169 (1996).
[5] G. Kresse and J. Hafner, Phys. Rev. B **49**, 14251 (1994).
[6] G. Kresse and J. Hafner, Phys. Rev. B **47**, 558 (1993).
[7] G. Kresse and D. Joubert, Phys. Rev. B **59**, 1758 (1999).
[8] P.E. Blöchl, Phys. Rev. B **50**, 17953 (1994).
[9] J.P. Perdew, J.A. Chevary, S.H. Vosko, K.A. Jackson, M.R. Pederson, D.J. Singh, and C. Fiolhais, Phys. Rev. B **46**, 6671 (1992).

[10] L. Wang, T. Maxisch, and G. Ceder, Phys. Rev. B **73**, 195107 (2006).
[11] A. Jain, G. Hautier, S.P. Ong, C.J. Moore, C.C. Fischer, K.A. Persson, and G. Ceder, Phys. Rev. B **84**, 045115 (2011).
[12] J. Ruiz-Fuertes, A. Friedrich, J. Pellicer-Porres, D. Errandonea, A. Segura, W. Morgenroth, E. Haussuhl, C.-Y. Tu, and A. Polian, Chem. Mater. **23**, 4220 (2011).
[13] C. Ederer and M. Komelj, Phys. Rev. B **76**, 064409 (2007).
[14] I. Efthimiopoulos, Z.T.Y. Liu, S. V Khare, P. Sarin, T. Lochbiler, V. Tsurkan, A. Loidl, D. Popov, and Y. Wang, Phys. Rev. B **92**, 064108 (2015).
[15] D. Das and S. Ghosh, J. Phys. D Appl. Phys. **48**, 425001 (2015).
[16] E. Winkler, S. Blanco-Canosa, F. Rivadulla, M.A. Lopez-Quintela, J. Rivas, A. Caneiro, M. T. Causa, and M. Tovar, Phys. Rev. B **80**, 104418 (2009).
[17] B.C. Melot, J.E. Drewes, R. Seshadri, E.M. Stoudenmire, and A.P. Ramirez, J. Phys. Cond. Matt. **21**, 216007 (2009).